

Precise radial velocities of giant stars. III.★

Spectroscopic stellar parameters

S. Hekker¹ and J. Meléndez²

¹ Leiden Observatory, Leiden University, P.O. Box 9513, 2300 RA Leiden, The Netherlands

² Research School of Astronomy & Astrophysics, Mount Stromlo Observatory, Cotter Road, Weston Creek, ACT 2611, Australia

Received |date|; accepted |date|

ABSTRACT

Context. A radial velocity survey of about 380 G and K giant stars is ongoing at Lick observatory. For each star we have a high signal to noise ratio template spectrum, which we use to determine spectroscopic stellar parameters.

Aims. The aim of this paper is to present spectroscopic stellar parameters, i.e. effective temperature, surface gravity, metallicity and rotational velocity for our sample of G and K giant stars.

Methods. Effective temperatures, surface gravities and metallicities are determined from the equivalent width of iron lines, by imposing excitation and ionisation equilibrium through stellar atmosphere models. Rotational velocities are determined from the full width at half maximum (FWHM) of moderate spectral lines. A calibration between the FWHM and total broadening (rotational velocity and macro turbulence) is obtained from stars in common between our sample and the sample from Gray (1989). Macro turbulence is determined from the macro turbulence vs. spectral type relations from Gray (2005).

Results. The metallicity we derive is essentially equal to the literature values, while the effective temperature and surface gravity are slightly higher by 56 K and 0.15 dex, respectively. A method comparison is performed with 72 giants in common with Luck and Heiter (2007), which shows that both methods give similar results. Our rotational velocities are comparable with those obtained by Gray (1989), but somewhat higher than those of de Medeiros & Mayor (1999), which is consistent with the different diagnostics used to determine them.

Conclusions. We are able to determine spectroscopic stellar parameters for about 380 G and K giant stars uniformly (112 stars are being analysed spectroscopically for the first time). For stars available in the literature, we find reasonable agreement between literature values and values determined in the present work. In addition, we show that the metallicity enhancement of companion hosting stars might also be valid for giant stars, with the planet hosting giants being 0.13 ± 0.03 dex (i.e. $35 \pm 10\%$) more metal rich than our total sample of stars.

Key words. stars: abundances – stars: fundamental parameters – stars: rotation – methods: observational – techniques: spectroscopic

1. Introduction

For the determination of spectroscopic stellar parameters, one needs high resolution spectra with high signal to noise ratio. These spectra are available from radial velocity surveys and are often used to determine stellar parameters. For instance, properties of cool stars from the Keck, Lick and AAT planet search are described by Valenti & Fischer (2005). Atmospheric parameters for stars observed by the N2K consortium (Fischer et al. 2005) are described by Robinson et al. (2007a). Santos et al. (2004, 2005) present stellar parameters and metallicities from the planet search using ESO facilities and the ELodie spectrograph at the 1.93 m telescope at the Observatoire de Haute Provence. Also, basic stellar parameters for 72 evolved stars, previously studied for radial velocity vari-

ations, are presented by da Silva et al. (2006). Some of these results are not only interesting in terms of the stellar parameters, but also reveal which stars are most likely to harbour sub-stellar companions. As first shown by Gonzalez (1997), and confirmed with larger samples by Fischer & Valenti (2005) and Santos et al. (2005), metal rich stars are more likely to harbour companions than metal poor ones.

Spectroscopic stellar parameters are most commonly determined by fitting the observed spectrum directly, see for instance Valenti & Fischer (2005), or by imposing excitation and ionisation equilibrium for metal lines, using an LTE analysis and a grid of model atmospheres, see for instance Santos et al. (2004, 2005), da Silva et al. (2006), Takeda et al. (2002) and Luck & Heiter (2007).

Rotational velocity and macro turbulence can only be determined directly with the Fourier transform technique, see for instance Gray (1989). Benz & Mayor (1981) have shown that accurate rotational velocities can also be deduced for dwarfs from

Send offprint requests to: S. Hekker,
email: saskia@strw.leidenuniv.nl

* Based on data obtained at UCO/Lick Observatory, USA.

a cross correlation function, by performing a calibration with the direct measurements of Gray (1989). de Medeiros & Mayor (1999) extended this technique for giant stars. Fekel (1997) used the full width at half maximum (FWHM) of weak to moderate spectral lines to determine rotational velocities, also by performing a calibration with the results of Gray (1989).

In 1999, a radial velocity survey of about 180 K giant stars was started at UCO/Lick Observatory, USA. This ongoing survey has recently been expanded to about 380 G and K giants. From the initial sample of 180 stars, companions have been announced for ι Draconis (Frink et al. 2002) and Pollux (Reffert et al. 2006). Stars with radial velocity variations of less than 20 ms^{-1} were presented as stable stars by Hekker et al. (2006), and an investigation into the mechanism(s) causing the radial velocity variations is presented by Hekker et al. (2007). Some binaries discovered with this survey, as well as an extensive overview of the sample, will be presented in forthcoming papers.

In this paper, we determine stellar parameters, i.e. effective temperature (T_{eff}), surface gravity ($\log g$) and metallicity ($[\text{Fe}/\text{H}]$), as well as rotational velocity ($v \sin i$) for all stars in the sample. In Sect. 2, we describe the observations. In Sects. 3 and 4, we present the methods used, and results for the stellar parameters and rotational velocity, respectively. In Sect. 5 a summary of our results is presented.

2. Observations

For the radial velocity survey, giants were selected from the Hipparcos catalog (Perryman & ESA 1997), based on the criteria described by Frink et al. (2001). The selected stars are all brighter than 6 mag, are presumably single and have photometric variations < 0.06 mag. These criteria are the same for the initial sample (K1 and later giants) as well as for the extension (G and K0, K1 giants). The survey started in 1999 at Lick observatory using the Coude Auxiliary Telescope (CAT) in conjunction with the Hamilton echelle spectrograph ($R = 60\,000$). The radial velocity measurements are performed with an iodine cell in the light path as described by Marcy & Butler (1992) and Valenti et al. (1995). Radial velocities are determined from the comparison of a stellar spectrum obtained with an iodine cell in the light path, and the convolution of a template iodine spectrum and a template stellar spectrum obtained without an iodine cell in the light path (Butler et al. 1996). For each target star we have a high signal to noise ratio template spectrum. These templates are used for the determination of the stellar parameters described in this paper. Thorium-Argon images taken at the beginning and end of each night are used for wavelength calibration.

3. Effective temperature, surface gravity, and metallicity

Spectroscopic stellar parameters (T_{eff} , $\log g$ and $[\text{Fe}/\text{H}]$) are determined by measuring the equivalent width (EW) of iron lines. The iron lines used in this work are listed in Table 1. The lines were carefully selected to avoid blends by atomic

Table 1. Iron lines considered in our analysis.

Ion	$\lambda [\text{\AA}]$	$\chi [\text{eV}]$	$\log gf$
Fe I	5775.080	4.220	-1.30
Fe I	5848.129	4.607	-0.9
Fe I	5902.473	4.593	-1.75
Fe I	5916.247	2.453	-2.99
Fe I	6027.050	4.076	-1.3
Fe I	6093.644	4.607	-1.41
Fe I	6096.665	3.984	-1.81
Fe I	6098.244	4.558	-1.8
Fe I	6120.249	0.915	-5.95
Fe I	6151.618	2.176	-3.30
Fe I	6187.990	3.943	-1.65
Fe I	6240.646	2.223	-3.39
Fe I	6498.939	0.958	-4.70
Fe I	6574.228	0.990	-5.00
Fe I	6703.567	2.759	-3.15
Fe I	6725.357	4.103	-2.30
Fe I	6726.666	4.607	-1.17
Fe I	7421.558	4.638	-1.80
Fe I	7547.896	5.099	-1.10
Fe I	7723.208	2.279	-3.62
Fe II	5264.812	3.230	-3.13
Fe II	5425.257	3.200	-3.22
Fe II	6247.557	3.892	-2.30
Fe II	6369.462	2.891	-4.11
Fe II	6432.680	2.891	-3.57
Fe II	6456.383	3.904	-2.05

and CN lines. CN blends were visually inspected by comparing a synthetic spectrum computed with laboratory CN lines (Meléndez & Barbuy 1999) with the high resolution visible atlas of the cool giant Arcturus (Hinkle et al. 2000). The $\log gf$ values are based on laboratory works, in some cases with small adjustments using the Arcturus atlas. For Fe I, they are from the Oxford group (e.g. Blackwell et al. 1995), Hannover group (e.g. Bard & Kock 1994), O'Brian et al. (1991), May et al. (1974) and Milford et al. (1994). For Fe II, the $\log gf$ values are from the laboratory normalisation performed by Meléndez et al. (2006).

It is very time consuming to determine EWs for about 380 stars by hand, using for instance the ‘splot’ routine from IRAF¹, we therefore used the publicly available Automatic Routine for line Equivalent widths in stellar Spectra (ARES) (Sousa et al. 2007). To check for possible differences between the EWs determined with ARES and those obtained with IRAF, we plot the EWs obtained with ARES vs. those obtained using IRAF (see Fig. 1). This comparison is done for a ‘hot’ ($T_{\text{eff}} = 4900$ K) and a ‘cool’ ($T_{\text{eff}} = 4050$ K) star in the sample. The mean differences between the EWs measured with ARES and IRAF are: $\langle \text{EW}_{\text{ARES}} - \text{EW}_{\text{IRAF}} \rangle = 1.6 \text{ m}\text{\AA}$ and $2.2 \text{ m}\text{\AA}$, with standard deviations of $6.6 \text{ m}\text{\AA}$ and $2.6 \text{ m}\text{\AA}$, for the ‘cool’ and ‘hot’ star respectively. The nearly 1 to 1 relation between the EWs obtained with both methods shows that it is reasonable

¹ IRAF is distributed by National Optical Astronomy Observatories, operated by the Association of Universities for Research in Astronomy, Inc., under contract with the National Science Foundation, U.S.A.

Table 2. Internal errors due to changes in stellar parameters for three stars with different temperatures. The total error in the last column includes the observational errors (0.024 dex for Fe I and 0.037 dex for Fe II).

Ion	ΔT_{eff} +80 K	$\Delta \log g$ +0.2 dex	Δv_t +0.2 km s $^{-1}$	$\sqrt{\sum x^2}$
HD156681 (T = 4170 K)				
Fe I	-0.01	+0.07	-0.07	0.10
Fe II	-0.15	+0.16	-0.03	0.22
HD214868 (T = 4445 K)				
Fe I	+0.01	+0.07	-0.06	0.10
Fe II	-0.12	+0.18	-0.04	0.22
HD165634 (T = 4980 K)				
Fe I	+0.06	+0.02	-0.06	0.09
Fe II	-0.06	+0.10	-0.07	0.14

to use EWs obtained with ARES. For some stars one or more lines appeared to be too strong (stronger than 200 mÅ) for a reliable parameter estimate. These lines are discarded.

From the EWs, stellar parameters are determined by imposing excitation and ionisation equilibrium through stellar atmosphere models. The micro turbulence (v_t) was obtained by requiring no dependence of Fe I against equivalent width. We performed a spectroscopic LTE analysis using the 2002 version of MOOG (Sneden 1973) and Kurucz model atmospheres, which include overshooting (Castelli et al. 1997). The resulting stellar parameters for each star are listed in Table 4 (only available in the online version). The reference solar iron abundance used in this study is $A(\text{Fe})_{\odot} = 7.49$ and was obtained using the same grid of Kurucz models.

Based on the scatter of the Fe lines, we obtained observational errors (standard errors) of 0.024 dex for Fe I and 0.037 dex for Fe II. Furthermore, we compute internal errors for a change of +80K, +0.2 dex and +0.2 km s $^{-1}$ in T_{eff} , $\log g$ and micro turbulence, respectively. The errors due to change in stellar parameters are shown for three stars with different temperatures in Table 2.

3.1. Comparison with the literature

We compare our spectroscopic stellar parameters with values obtained from the literature. These literature values are from an updated version (Ramírez & Meléndez 2005) of the Cayrel de Strobel et al. (2001) [Fe/H] catalogue (254 stars in common), including the Luck & Heiter (2007) catalogue. If possible, suspicious literature values were corrected according to the normalisation suggested by Taylor (1999). In Fig. 2 the difference between our spectroscopic and literature values are plotted for the temperature, surface gravity and metallicity. We find the following trimean difference and pseudo-sigma for the stellar parameters:

$$\begin{aligned} <[\text{Fe}/\text{H}]^{\text{spec}} - [\text{Fe}/\text{H}]^{\text{lit}}> &= 0.01 \text{dex} & \sigma &= 0.10 \text{dex} \\ <\log g^{\text{spec}} - \log g^{\text{lit}}> &= 0.15 \text{dex} & \sigma &= 0.22 \text{dex} \\ < T_{\text{eff}}^{\text{spec}} - T_{\text{eff}}^{\text{lit}}> &= 56 \text{K} & \sigma &= 84 \text{K} \end{aligned}$$

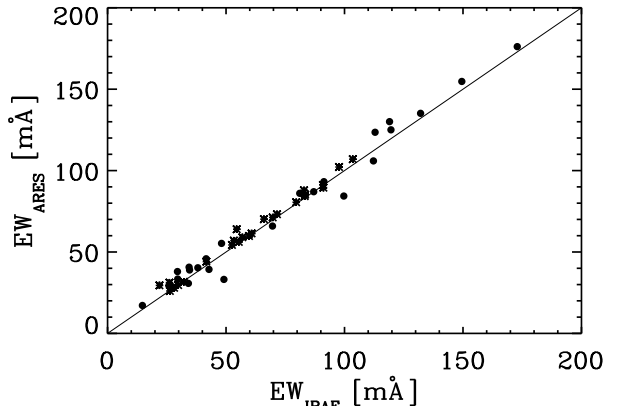


Fig. 1. EWs obtained with the ARES software as a function of EWs computed using IRAF. The dots indicate a star with $T_{\text{eff}} = 4050$ K ('cool') and the asterisks a star with $T_{\text{eff}} = 4900$ K ('hot'). The solid line is a 1 to 1 relation.

The trimean T is a robust estimate of central tendency: $T=(Q1+2 \times \text{median}+Q3)/4$ where Q1 and Q3 are the first and third quartile. The pseudo-standard deviation σ is obtained from the quartile deviation $QD = (Q3-Q1)/2$, employing $\sigma = 3/2 QD$ (Meléndez et al. 2006).

The difference in our spectroscopic metallicity and the literature value is essentially zero and we conclude that our metallicity scale is correct. Furthermore, our T_{eff} values are in good agreement with the literature, with a scatter of only 84 K, and a zero point difference of 56 K, our T_{eff} values being higher than the values in the literature. From the left panel of Fig. 2 one can see that the difference is largest for the coolest stars in the sample. This might be due to the fact that the models are less accurate for low temperatures. In addition, the number of spectral lines increases with decreasing temperature, the spectra might be too crowded at lower temperatures, and also the lines get stronger and more dependent on the micro turbulence. Our results below 4000 K should be interpreted with caution.

The spectroscopic gravities we derived also agree well with the literature, with a scatter of only 0.22 dex, and a zero point difference of 0.15 dex. We checked whether the enhanced $\log g$ values from our spectroscopic analyses are related to the higher temperatures we obtained, compared to literature values. We therefore performed a test for three stars with T_{eff} 4170 K, 4445 K and 4980 K, respectively. We increased T_{eff} with 100 K and determined $\log g$, while keeping the micro turbulence fixed. For all three stars we obtained higher $\log g$ values for the increased temperatures. This reveals that the higher values for $\log g$, compared to the literature values, are related to the higher effective temperatures.

3.2. Comparison with Luck & Heiter (2007)

Recently, Luck & Heiter (2007) presented a homogeneous spectroscopic analysis of 298 giants in the local region, using between 300 and 400 Fe I lines for each star and MARCS stellar models (Gustafsson et al. 2003) on spectra with $R=60\,000$.

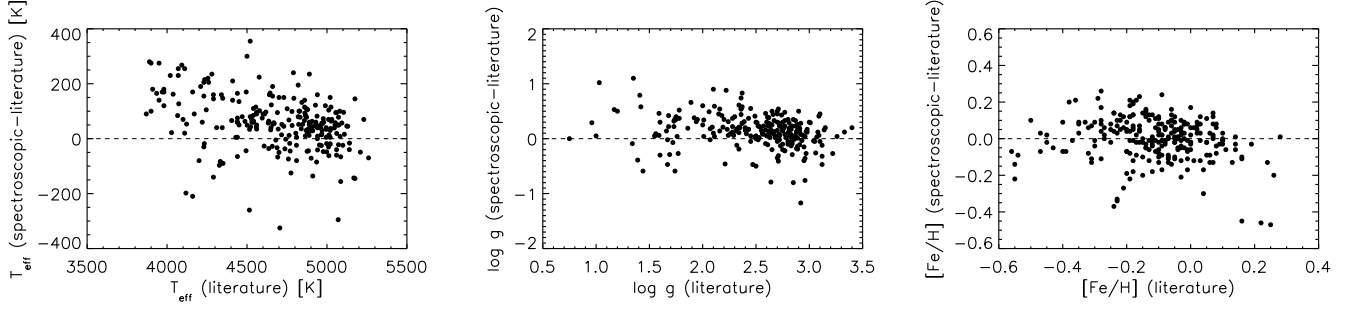


Fig. 2. Difference between our spectroscopic values and literature values as a function of literature values for the effective temperature (left), the logarithm of the surface gravity in cgs units (centre) and metallicity (right).

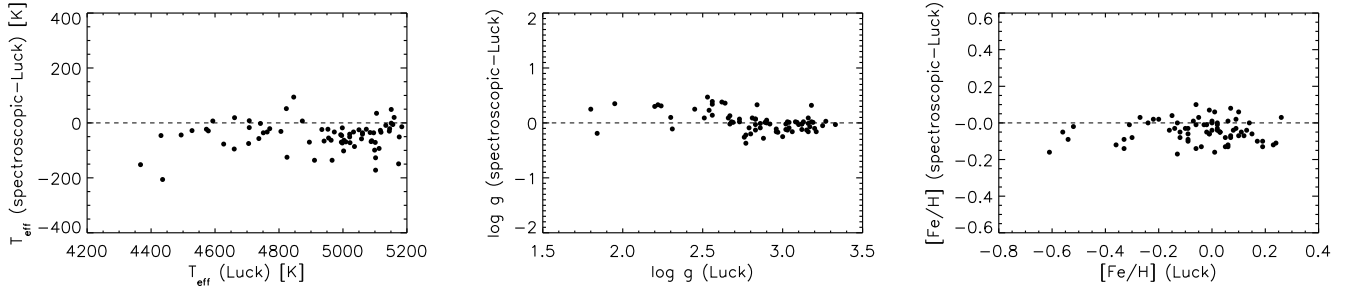


Fig. 3. Difference between our spectroscopic values and values from Luck & Heiter (2007) as a function of Luck & Heiter (2007) values for the effective temperature (left), the logarithm of the surface gravity in cgs units (centre) and metallicity (right) for the 72 stars in common between the samples.

We used the 72 stars in common between Luck & Heiter (2007) and our sample, to see how well we can determine spectroscopic stellar parameters with just two dozen carefully selected iron lines instead of a few hundred iron lines. Note that different models are used for the two analyses, however spectra have the same resolution. A comparison for each parameter is shown in Fig. 3. We find the following trimean difference and pseudo-sigma:

$$\begin{aligned} <[\text{Fe}/\text{H}]^{\text{spec}} - [\text{Fe}/\text{H}]^{\text{Luck}}> &= -0.05 \text{dex} \quad \sigma = 0.06 \text{dex} \\ <\log g^{\text{spec}} - \log g^{\text{Luck}}> &= 0.0 \text{dex} \quad \sigma = 0.15 \text{dex} \\ < T_{\text{eff}}^{\text{spec}} - T_{\text{eff}}^{\text{Luck}}> &= -43 \text{K} \quad \sigma = 35 \text{K} \end{aligned}$$

Our spectroscopic values are in good agreement with those obtained by Luck & Heiter (2007), with a scatter of only 0.06 dex for [Fe/H], 0.15 dex for $\log g$ and 35 K for the effective temperature. The mean difference in $\log g$ values is zero, while our metallicities and temperatures are slightly lower than those reported by Luck & Heiter (2007). These are probably systematic differences between both methods, because the pseudo-sigmas are relatively small. Luck & Heiter (2007) have benchmarked their codes against Kurucz's WIDTH and SYNTHE codes and claim that all codes yield the same result to within expected numerical accuracy and differences due to different assumptions, primarily partition functions and damping. It is therefore likely that the different adopted model atmospheres (MARCS vs. Kurucz) and different $\log gf$ values cause the small systematic difference. Luck & Heiter (2007) did not publish their line list and $\log gf$ values. Since they have used a much larger num-

ber of iron lines a comparison with our $\log gf$ values is probably not meaningful.

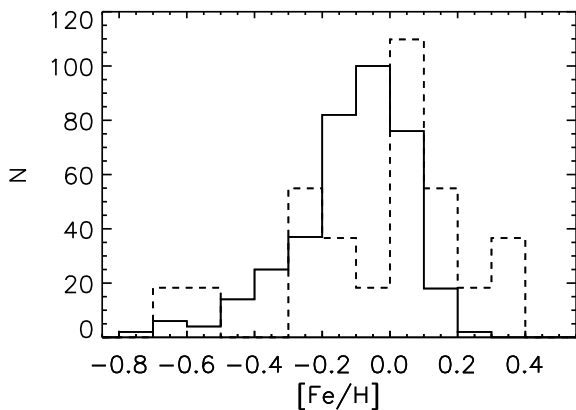
3.3. Metallicity in companion hosting giants

By now 20 sub-stellar companions are announced as orbiting giant stars. Some recent publications, e.g. Sadakane et al. (2005) and Pasquini et al. (2007), suggest that giant stars with companions are metal poor, which is quite different from the known metallicity enhancement in dwarf stars hosting companions. Schuler et al. (2005) and da Silva et al. (2006) argue that giant stars with companions may be metal poor, due to a stellar mass-companion relation instead of a metallicity-companion relation. Indeed, Fischer & Valenti (2005) also find a relation between stellar mass and companions, but conclude that this is likely spurious. Here, we look at the metallicities of the giants with announced companions and compare these with the metallicities of the giants in our sample. For consistency with our work, the companion hosting giants are selected to encompass the same range in stellar parameters as our sample of giants, i.e. stars with $T_{\text{eff}} \approx 4600 \pm 750$ K and $\log g \approx 2.1 \pm 1.5$.

The companion hosting giants and their metallicities adopted for the comparison are listed in Table 3. In order to perform a homogeneous comparison between the metallicities of the total and the companion hosting giant sample we determined the metallicity zero-points of the literature works we are using for the companion hosting giant stars. We found the following zero-points: -0.05 dex for Luck & Heiter (2007), -0.10 dex for Schuler et al. (2005), -0.02 dex for

Table 3. Companion hosting giants with their mean metallicities and literature sources.

HIP	HD	[Fe/H]	literature
4297	5319	+0.04	Robinson et al. (2007b)
8928	11977	-0.19	da Silva et al. (2006), Sousa et al. (2006)
10085	13189	-0.57	Schuler et al. (2005), Sousa et al. (2006)
	17092	+0.19	Niedzielski et al. (2007)
19921	27442	+0.33	Santos et al. (2003), Valenti & Fischer (2005)
20889	28305	+0.10	Mishenina et al. (2006), Schuler et al. (2006), Sato et al. (2007), this work
31688	47536	-0.64	Sadakane et al. (2005), da Silva et al. (2006)
36616	59686	+0.11	Santos et al. (2005), Sadakane et al. (2005), Mishenina et al. (2006), this work
37826	62509	+0.06	Sadakane et al. (2005), Luck & Heiter (2007), this work
42527	73108	-0.24	Luck & Heiter (2007), Doellinger et al. (2007)
58952	104985	-0.29	Santos et al. (2005), Takeda et al. (2005), Luck & Heiter (2007)
68581	122430	-0.10	da Silva et al. (2006)
75458	137759	+0.07	Santos et al. (2003), Sadakane et al. (2005), this work
92895	175541	-0.18	Valenti & Fischer (2005)
93746	177830	+0.35	Santos et al. (2003), Valenti & Fischer (2005)
99894	192699	-0.26	Johnson et al. (2007)
109577	210702	+0.01	Luck & Heiter (2007), Johnson et al. (2007)
114855	219449	0.00	Santos et al. (2005), Sadakane et al. (2005), Luck & Heiter (2007), this work
116727	222404	+0.21	Luck & Heiter (2007)
NGC 2423-3	BD-13 2130	+0.06	Twarog et al. (1997)

**Fig. 4.** Distribution of metallicities of all stars in our sample with mean, median and trimean values of -0.12 , -0.09 and -0.095 dex, respectively. The metallicity of 20 giants with an announced companion in the literature (see text for selection criteria) are plotted with the dashed histogram. The latter distribution is normalised to the total number of giants in our sample. These giants have mean, median and trimean metallicity values of -0.05 , $+0.025$ and -0.015 dex, respectively.

da Silva et al. (2006) and Doellinger et al. (2007), -0.07 dex for Santos et al. (2003, 2005) and Sousa et al. (2006), -0.11 dex for Johnson et al. (2007), Valenti & Fischer (2005) and Robinson et al. (2007b), 0.00 dex for Mishenina et al. (2006), -0.05 dex for Sadakane et al. (2005), Sato et al. (2007) and Takeda et al. (2005), and -0.85 dex for Twarog et al. (1997). Note that Twarog et al. (1997) only provide a mean metallicity for the cluster NGC 2423 based on photometry. The normalisation factor is based on the Hyades. For Niedzielski et al. (2007) we do not have any stars in common, so we adopted a

zero-point of $+0.01$ dex, which we obtained from the global comparison with the literature. In the event that more individual measurements of a star were available in the literature, the mean metallicity was adopted. The literature sources are mentioned in the last column of Table 3.

In Fig. 4 the metallicity distribution of all stars in the present sample is shown together with the metallicity distribution of giant stars with announced companions. The companion hosting giant star distribution shows a gap at -0.1 dex. We do not know whether this gap is real or due to low number statistics. The mean, median and trimean metallicities are -0.12 , -0.09 and -0.095 dex and -0.05 , $+0.025$ and -0.015 dex for the total and companions hosting sample, respectively, while the peaks of the histograms are at -0.05 dex and $+0.05$ dex. Gaussians fitted through the two distribution have their centres at -0.06 dex and $+0.09$ dex ($+0.085$ dex in case one Gauss is fitted and $+0.09$ for 2 Gaussian fits) for the total and companion hosting sample, respectively. Therefore, the metallicity enhancement for companion hosting giants is 0.13 ± 0.03 dex. This is similar to the metallicity enhancement found by Fischer & Valenti (2005). Their comparison between metallicities of all stars in the sample and companion hosting dwarfs reveals that companion hosting dwarfs are more metal rich by 0.13 dex. If they compare the metallicity enhancement as a function of stellar mass, they find also that, independent of mass, the metallicity distribution of dwarfs with companions is 0.12 dex higher than the average metallicity of all stars in the sample.

Although the determination of precise stellar masses, for both our sample of field giant stars and the companion hosting giant stars, is beyond the scope of the present paper, we stress that overall both samples have comparable masses. Using the masses given by Allende Prieto & Lambert (1999), we estimate a typical mass of $2.0 M_{\odot}$ for our sample, with the bulk

of the field giant sample in the range $1.4 - 2.9 M_{\odot}$ (first to third quartiles), which is the typical range covered by companion hosting giants according to Sadakane et al. (2005) and Johnson et al. (2007).

The metallicity enhancement for companion hosting giants should be taken with caution. First, it is still based on low number statistics. Second, for nearly 200 stars in our sample, we do not have a long enough time span of radial velocity observations to detect companions, in case these are present. Third, there is still some discussion ongoing about some of the companion hosting giants with companions in (nearly) circular orbits. The observed radial velocity variations could in principle also be due to a mechanism intrinsic to the star.

The present conclusion that companion hosting giants are on average metal rich is rather different compared to other studies. Sadakane et al. (2005) and Pasquini et al. (2007) both agree that the giant stars with companions are typically not much more metal rich than $[Fe/H] = 0.0$. Sadakane et al. (2005) analysed only a few giants, therefore their results may be due to statistics based on small numbers. However, Pasquini et al. (2007) used a total of 14 giants, slightly less than our sample of 20 giants. The two samples have only 10 stars in common (HD11977, HD13189, HD28305, HD47536, HD62509, HD73108, HD104985, HD122430, HD137759, HD222404), which include the most metal poor giants in the sample, but does not contain some of the more metal rich ones. Since their histogram for the companion hosting giants does not include stars with $[Fe/H] > +0.2$ dex, we suspect that the four candidates which are not available in the literature are also not as metal rich as for example HD27442 and HD177830, both with $[Fe/H] > +0.3$ (Santos et al. (2003); Valenti & Fischer (2005)). Note that Pasquini et al. (2007) did not correct for potential systematic errors in the literature $[Fe/H]$ values for giant stars with companions.

Finally, caution should be taken when comparing dwarfs with giants, since systematic errors are expected due to differences in their atmospheric structures and parameters (Asplund 2005). Indeed, in a large study of several hundreds of giants and dwarfs, Luck & Heiter (2007) show that the abundances of Fe, Mn and Ba in giants may be affected by systematic uncertainties when compared with dwarf stars. A consistent study such as ours, comparing field giants to companion hosting giants, is therefore more reliable.

4. Rotational velocity

We computed rotational velocities for our sample of giant stars, using the method described by Fekel (1997). The FWHM for moderate spectral lines at 6432.68, 6452.33, 6454.99, 6455.60, 6456.38, 6469.15 and 6471.66 Å is determined and averaged. The dispersion of the FWHM resulting from individual lines is typically 0.025 mÅ. The instrumental broadening is determined from Thorium-Argon (ThAr) images taken at the beginning and end of each night. The FWHM of several ThAr lines, in the same spectral region as the stellar lines, are determined and averaged. The intrinsic stellar broadening is computed as

$$FWHM_{intrinsic} = \sqrt{FWHM_{measured}^2 - FWHM_{instrumental}^2}.$$

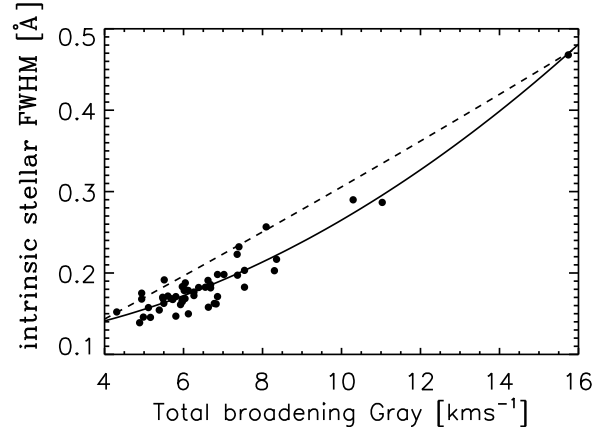


Fig. 5. The intrinsic stellar FWHM of spectral lines as a function Gray's total broadening, for 51 stars in common between our sample and Gray (1989). The best fit (Equation [1]) is shown as the solid line, while the best fit obtained by Fekel (1997) is shown as the dashed line.

The intrinsic stellar broadening is converted to rotational velocity $v \sin i$, using the results from Gray (1989). For the 51 stars in common (excluding 2 outliers, for which we find higher velocities than Gray 1989), the intrinsic broadening is plotted as a function of the total broadening ($\sqrt{(v \sin i)^2 + v_{macro}^2}$) determined by Gray (1989), as shown in Fig. 5. A second order polynomial is fitted:

$$FWHM_{intrinsic} = 0.10963 + 0.002758X + 0.001278X^2, \quad (1)$$

with X the value of Gray's total broadening. The dispersion of this fit is 0.015 Å. This fit is used as calibration to convert the $FWHM_{intrinsic}$ in Å to total broadening in km s^{-1} . Note that we only cover a total broadening between 4 and 16 km s^{-1} . All stars in our sample fall in this range. Furthermore, our fit in Fig. 5 is different from that of Fekel (1997), which is shown in Fig. 5 with the dashed line. Fekel (1997) covers a much wider range in total broadening and might not be sensitive to the curvature in the particular region discussed here. In this study we used Eq. (1) to derive the total broadening in km s^{-1} . From this total broadening we derive the rotational velocity as $v \sin i = \sqrt{FWHM_{total}^2 - v_{macro}^2}$.

4.1. Macro turbulence

The macro turbulence is derived from the spectral type as shown in Figure 17.10 from Gray (2005). Each luminosity class has its own relation. We estimate the luminosity class from a $\log g$ vs. T_{eff} relation (Fig. 6). Most stars in the sample are luminosity class III stars, and therefore, the second order best fit relation, shown in Eq. (2), is used for class III stars. This relation has a robust sigma scatter of 0.25 dex.

$$\log g_{III} = -26.332 + 1.117 \cdot 10^{-2} T_{\text{eff}} - 1.064 \cdot 10^{-6} T_{\text{eff}}^2. \quad (2)$$

Stars within a factor of 2 of the $\log g_{III}$ relation are considered to be class III giants, resulting in the following subdivision:

$$\text{giants: } \log g = \log g_{III} \pm 0.3 \text{ dex},$$

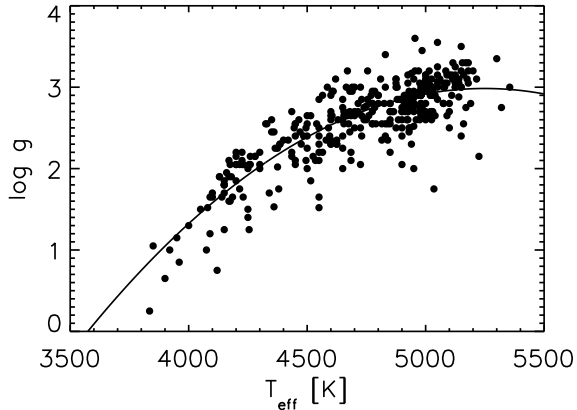


Fig. 6. Log g vs. T_{eff} for all stars in our sample. The solid line shows the best fit (Eq. [2]).

$$\begin{aligned} \text{subgiants: } & \log g > \log g_{III} + 0.3 \text{ dex}, \\ \text{luminous giants: } & \log g < \log g_{III} - 0.3 \text{ dex}. \end{aligned}$$

With the luminosity classes, we used Figure 17.10 from Gray (2005) to determine relations between v_{macro} and T_{eff} for luminosity classes II, III and IV. We found the following relations:

$$\begin{aligned} \text{class II: } v_{\text{macro}} &= -0.214 + 0.00158T_{\text{eff}} \quad \sigma = 0.55 \text{ kms}^{-1} \quad (3) \\ \text{class III: } v_{\text{macro}} &= -3.953 + 0.00195T_{\text{eff}} \quad \sigma = 0.45 \text{ kms}^{-1} \quad (4) \\ \text{class IV: } v_{\text{macro}} &= -8.426 + 0.00241T_{\text{eff}} \quad \sigma = 0.23 \text{ kms}^{-1} \quad (5) \end{aligned}$$

In the case that v_{macro} appeared to be higher than the total broadening, we used v_{macro} from a higher luminosity class to determine $v \sin i$. In case v_{macro} was still too high, we adopted $v_{\text{macro}} = 3 \text{ kms}^{-1}$, as used by Fekel (1997) for G and K giants.

4.2. Comparison with the literature

We checked our final $v \sin i$ values by comparing the values of the 51 stars in common between our sample and Gray (1989), see Fig. 7. The values are located around the 1 to 1 relation indicated by the solid line, which shows that the results of both samples are consistent. We also have 184 stars in common with de Medeiros & Mayor (1999) and compare our $v \sin i$ values with theirs in Fig. 8. Our values are on average higher than those obtained by de Medeiros & Mayor (1999). This is probably due to the different diagnostics used. de Medeiros & Mayor (1999) show that the relation between their $v \sin i$ values, and those obtained by Gray (1989) for class III and IV, has an offset of 1.15 and a correlation coefficient of 1.18. We plotted the 1 to 1 relation, solid line, as well as the relation between $v \sin i$ obtained by Gray (1989) and de Medeiros & Mayor (1999) in Fig. 8, dashed line. The data are located around this latter relation. This indicates that the difference between the results obtained here and from de Medeiros & Mayor (1999) are due to the different diagnostics used to determine $v \sin i$. Also, Luck & Heiter (2007) find that the CORAVEL $v \sin i$ values may suffer from systematic differences with respect to values

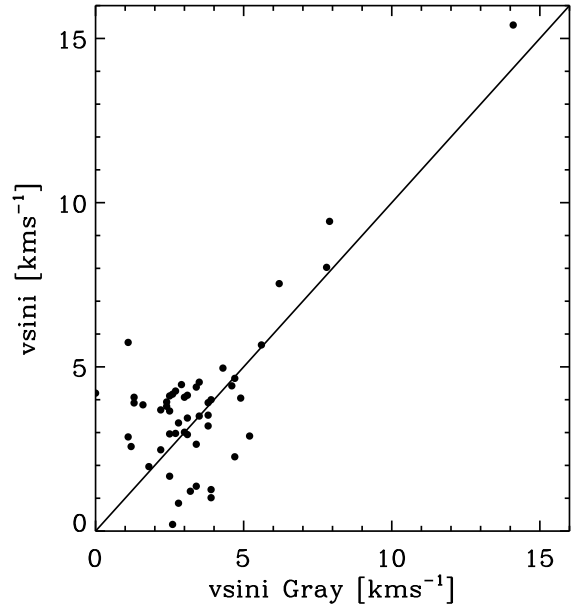


Fig. 7. $v \sin i$ obtained here vs. $v \sin i$ obtained by Gray (1989). The solid line is a 1 to 1 relation.

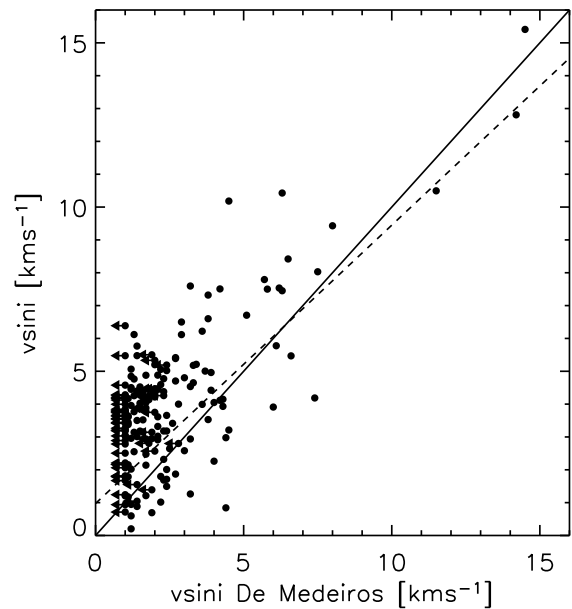


Fig. 8. $v \sin i$ obtained here vs. $v \sin i$ obtained by de Medeiros & Mayor (1999). The solid line is a 1 to 1 relation and the dashed line is the relation between $v \sin i$ obtained by Gray (1989) and de Medeiros & Mayor (1999). The arrows indicate upper limits.

derived from other techniques. For all stars $v \sin i$ and v_{macro} are listed in Table 4 (only available in the online version).

5. Summary

We have determined spectroscopic stellar parameters for a sample of about 380 G and K giant stars. Among these, 112 stars are analysed spectroscopically for the first time. Our metallicities agree with values found in the literature and we conclude that our metallicity scale is not severely affected by systematic errors. Our temperatures are ~ 50 K higher compared to those from the literature. The difference is largest for stars with lowest temperatures. This is probably due to the lower accuracy of atmosphere models in this temperature range, the increased number and strength of spectral lines and increasing dependence on micro turbulence in cooler stars. An increase in temperature causes an increase in surface gravity and our values are 0.15 dex higher compared to the literature values.

The comparison between the mean metallicity of our total sample of giant stars and giant stars with announced companions reveals that the companion hosting stars have a 0.13 ± 0.03 dex higher metallicity than the mean metallicity of our total sample. This is in agreement with the enhanced metallicity of companion hosting dwarf stars, but is based on low number statistics.

Rotational velocities are determined using the method described by Fekel (1997). Stars in common between our sample and that observed by Gray (1989) are used to convert FWHM of moderate lines [Å] to total line broadening [km s^{-1}]. We used a $\log g$ vs. T_{eff} correlation to determine the luminosity class of the stars. This luminosity class was subsequently used to calculate the macro turbulence, which has a different relation with temperature for different classes. Our data are in agreement with those obtained by Gray (1989), but are on average larger than the values obtained by de Medeiros & Mayor (1999). This is due to the different diagnostics used to determine $v \sin i$.

Acknowledgements. We are very grateful to Andreas Quirrenbach, Sabine Reffert and Dave Mitchell, who started the radial velocity survey of giant stars, to allow us to use the template spectra for the present analysis. We also want to thank Conny Aerts and Ignas Snellen for carefully reading the manuscript and useful discussions. We would like to thank the referee for carefully reading the manuscript and constructive comments.

References

- Allende Prieto, C. & Lambert, D. L. 1999, A&A, 352, 555
 Asplund, M. 2005, ARA&A, 43, 481
 Bard, A. & Kock, M. 1994, A&A, 282, 1014
 Benz, W. & Mayor, M. 1981, A&A, 93, 235
 Blackwell, D. E., Lynas-Gray, A. E., & Smith, G. 1995, A&A, 296, 217
 Butler, R. P., Marcy, G. W., Williams, E., et al. 1996, PASP, 108, 500
 Castelli, F., Gratton, R. G., & Kurucz, R. L. 1997, A&A, 324, 432
 Cayrel de Strobel, G., Soubiran, C., & Ralite, N. 2001, A&A, 373, 159
 da Silva, L., Girardi, L., Pasquini, L., et al. 2006, A&A, 458, 609
 de Medeiros, J. R. & Mayor, M. 1999, A&AS, 139, 433
 Doellinger, M., Hatzes, A., Pasquini, L., et al. 2007, in astroph, 3672 (2007), 3672
 Fekel, F. C. 1997, PASP, 109, 514
 Fischer, D. A., Laughlin, G., Butler, P., et al. 2005, ApJ, 620, 481
 Fischer, D. A. & Valenti, J. 2005, ApJ, 622, 1102
 Frink, S., Mitchell, D. S., Quirrenbach, A., et al. 2002, ApJ, 576, 478
 Frink, S., Quirrenbach, A., Fischer, D., Röser, S., & Schilbach, E. 2001, PASP, 113, 173
 Gonzalez, G. 1997, MNRAS, 285, 403
 Gray, D. F. 1989, ApJ, 347, 1021
 Gray, D. F. 2005, The Observation and Analysis of Stellar Photospheres (The Observation and Analysis of Stellar Photospheres, 3rd Edition, by D.F. Gray. ISBN 0521851866. Cambridge, UK: Cambridge University Press, 2005.)
 Gustafsson, B., Edvardsson, B., Eriksson, K., et al. 2003, in Astronomical Society of the Pacific Conference Series, Vol. 288, Stellar Atmosphere Modeling, ed. I. Hubeny, D. Mihalas, & K. Werner, 331
 Hekker, S., Reffert, S., Quirrenbach, A., et al. 2006, A&A, 454, 943
 Hekker, S., Snellen, I., Aerts, C., et al. 2007, A&A, in preparation
 Hinkle, K., Wallace, L., Valenti, J., & Harmer, D. 2000, Visible and Near Infrared Atlas of the Arcturus Spectrum 3727-9300 Å (Visible and Near Infrared Atlas of the Arcturus Spectrum 3727-9300 Å ed. Kenneth Hinkle, Lloyd Wallace, Jeff Valenti, and Dianne Harmer. (San Francisco: ASP) ISBN: 1-58381-037-4, 2000.)
 Johnson, J. A., Fischer, D. A., Marcy, G. W., et al. 2007, ApJ, 665, 785
 Luck, R. E. & Heiter, U. 2007, AJ, 133, 2464
 Marcy, G. W. & Butler, R. P. 1992, PASP, 104, 270
 May, M., Richter, J., & Wichelmann, J. 1974, A&AS, 18, 405
 Meléndez, J. & Barbuy, B. 1999, ApJS, 124, 527
 Meléndez, J., Shchukina, N. G., Vasiljeva, I. E., & Ramírez, I. 2006, ApJ, 642, 1082
 Milford, P. N., O'Mara, B. J., & Ross, J. E. 1994, A&A, 292, 276
 Mishenina, T. V., Bienaymé, O., Gorbaneva, T. I., et al. 2006, A&A, 456, 1109
 Niedzielski, A., Konacki, M., Wolszczan, A., et al. 2007, ArXiv e-prints, 705
 O'Brian, T. R., Wickliffe, M. E., Lawler, J. E., Whaling, J. W., & Brault, W. 1991, Journal of the Optical Society of America B Optical Physics, 8, 1185
 Pasquini, L., Doellinger, M. P., Weiss, A., et al. 2007, ArXiv e-prints, 707
 Perryman, M. A. C. & ESA. 1997, The HIPPARCOS and TYCHO catalogues. Astrometric and photometric star catalogues derived from the ESA HIPPARCOS Space

Astrometry Mission (The Hipparcos and Tycho catalogues. Astrometric and photometric star catalogues derived from the ESA Hipparcos Space Astrometry Mission, Publisher: Noordwijk, Netherlands: ESA Publications Division, 1997, Series: ESA SP Series vol no: 1200, ISBN: 9290923997 (set))

Ramírez, I. & Meléndez, J. 2005, ApJ, 626, 446

Reffert, S., Quirrenbach, A., Mitchell, D. S., et al. 2006, ApJ, 652, 661

Robinson, S. E., Ammons, S. M., Kretke, K. A., et al. 2007a, ApJS, 169, 430

Robinson, S. E., Laughlin, G., Vogt, S. S., et al. 2007b, ArXiv e-prints, 708

Sadakane, K., Ohnishi, T., Ohkubo, M., & Takeda, Y. 2005, PASJ, 57, 127

Santos, N. C., Israelian, G., & Mayor, M. 2004, A&A, 415, 1153

Santos, N. C., Israelian, G., Mayor, M., et al. 2005, A&A, 437, 1127

Santos, N. C., Israelian, G., Mayor, M., Rebolo, R., & Udry, S. 2003, A&A, 398, 363

Sato, B., Izumiura, H., Toyota, E., et al. 2007, ApJ, 661, 527

Schuler, S. C., Hatzes, A. P., King, J. R., Kürster, M., & The, L.-S. 2006, AJ, 131, 1057

Schuler, S. C., Kim, J. H., Tinker, Jr., M. C., et al. 2005, ApJ, 632, L131

Sneden, C. A. 1973, PhD thesis, AA(The University of Texas in Austin.)

Sousa, S. G., Santos, N. C., Israelian, G., Mayor, M., & Monteiro, M. J. P. F. G. 2006, A&A, 458, 873

Sousa, S. G., Santos, N. C., Israelian, G., Mayor, M., & Monteiro, M. J. P. F. G. 2007, A&A, 469, 783

Takeda, Y., Ohkubo, M., & Sadakane, K. 2002, PASJ, 54, 451

Takeda, Y., Sato, B., Kambe, E., et al. 2005, PASJ, 57, 109

Taylor, B. J. 1999, A&AS, 134, 523

Twarog, B. A., Ashman, K. M., & Anthony-Twarog, B. J. 1997, AJ, 114, 2556

Valenti, J. A., Butler, R. P., & Marcy, G. W. 1995, PASP, 107, 966

Valenti, J. A. & Fischer, D. A. 2005, ApJS, 159, 141

Table 4. Stellar parameters: Star name, V magnitude, parallax (plx) in mas with its error (e_plx), B-V colour, all from the Hipparcos catalogue (Perryman & ESA 1997), effective temperature (T_{eff}) in Kelvin, surface gravity ($\log g$) in dex, micro turbulence (ξ) in km s^{-1} , metallicity (A(Fe)), rotational velocity ($v \sin i$) in km s^{-1} and macro turbulence (v_{macro}) in km s^{-1} .

HIP	HD	V mag	plx mas	e_plx mas	B-V mag	T_{eff} K	$\log g$ dex	ξ km s^{-1}	A(Fe)	$v \sin i$ km s^{-1}	v_{macro} km s^{-1}
379	225216	5.68	10.30	0.58	1.051	4775	2.8	1.75	7.42	0.71	5.36
1354	1239	5.74	5.08	0.58	0.898	5150	2.4	1.81	7.23	0.84	7.92
1562	1522	3.56	11.26	0.73	1.214	4500	2.25	2.0	7.52	3.37	4.82
2006	2114	5.77	5.50	1.03	0.855	5160	2.55	1.85	7.36	1.26	6.11
2497	2774	5.59	8.29	0.68	1.163	4550	2.85	1.8	7.42	3.66	2.54
2942	3421	5.45	3.19	0.77	0.886	5225	2.15	2.57	7.14	5.51	8.04
3031	3546	4.34	19.34	0.76	0.871	4975	2.6	1.65	6.88	4.12	3.56
3179	3712	2.24	14.27	0.57	1.170	4625	2.30	2.85	7.29	6.71	5.07
3193	3807	5.90	5.66	0.94	1.091	4625	2.3	1.76	7.05	1.81	5.07
3231	3817	5.30	9.47	0.81	0.891	5025	2.65	1.5	7.34	1.21	5.85
3419	4128	2.04	34.04	0.82	1.019	4925	3.05	2.2	7.40	4.07	5.65
3607	4398	5.49	9.78	0.71	0.978	4925	2.7	1.66	7.30	2.27	5.65
3760	4627	5.92	4.93	0.82	1.104	4600	2.3	1.78	7.24	3.96	2.66
4422	5395	4.62	15.84	0.58	0.957	4860	2.7	1.64	7.09	2.16	3.29
4510	5575	5.44	4.63	0.74	1.076	4725	2.05	2.23	7.24	11.27	7.25
4587	5722	5.62	10.35	0.96	0.949	4925	2.7	1.41	7.31	4.44	3.44
4906	6186	4.27	17.14	0.81	0.952	4900	2.7	1.6	7.25	3.54	3.38
4914	6203	5.40	7.95	0.86	1.106	4650	2.6	1.54	7.22	2.72	5.11
5364	6805	3.46	27.73	0.71	1.161	4600	2.9	1.85	7.56	3.78	2.66
5571	7087	4.66	7.42	0.68	1.024	4850	2.55	1.77	7.34	3.54	5.50
5742	7318	4.67	8.64	0.81	1.047	4815	2.55	1.92	7.38	6.22	5.44
6537	8512	3.60	28.48	0.77	1.065	4750	2.77	1.8	7.36	3.61	3.02
6732	8763	5.50	10.63	0.77	1.106	4690	3.0	1.95	7.48	4.46	2.88
6999	9057	5.27	11.26	0.77	0.999	4950	2.8	1.58	7.55	4.47	3.50
7607	9927	3.59	18.76	0.74	1.275	4375	2.25	1.85	7.56	2.78	4.58
7884	10380	4.45	8.86	0.77	1.347	4300	2.2	2.25	7.22	3.00	4.43
7906	10348	5.97	6.23	0.80	1.015	4885	2.6	1.8	7.43	5.50	5.57
8198	10761	4.26	12.63	0.86	0.942	5025	2.9	1.75	7.49	4.46	3.68
9110	11909	5.09	4.95	0.95	0.921	5025	2.6	1.8	7.39	3.33	7.73
9347	12274	3.99	10.84	0.79	1.554	4200	2.2	2.35	7.43	7.52	1.70
9631	12641	5.96	9.89	0.88	0.851	4875	3.1	1.42	7.34	7.61	5.55
9884	12929	2.01	49.48	0.99	1.151	4600	2.7	1.7	7.36	3.44	2.66
10234	13468	5.94	9.20	0.83	0.967	4925	2.8	1.44	7.37	0.19	5.65
10326	13692	5.86	8.17	0.81	1.006	4970	3.2	1.53	7.52	3.64	3.55
10642	14129	5.51	9.58	0.93	0.962	5000	3.05	1.79	7.42	4.00	3.62
10729	13994	5.99	4.59	0.69	1.039	4935	2.5	2.04	7.29	10.49	7.58
11220	14770	5.19	8.69	0.67	0.979	4985	2.75	1.68	7.46	0.69	5.77
11432	15176	5.55	11.39	1.04	1.114	4650	2.85	1.65	7.42	3.60	2.78
12093	16161	4.87	8.77	1.11	0.880	5170	2.75	1.62	7.31	4.70	6.13
13288	17824	4.76	17.85	0.69	0.906	5180	3.3	1.3	7.56	3.66	4.06
13339	17656	5.86	8.21	0.79	0.903	5150	3.0	1.37	7.53	2.91	6.09
13701	18322	3.89	24.49	0.72	1.088	4700	3.00	1.58	7.46	2.92	2.90
13905	18449	4.94	9.31	0.78	1.235	4500	2.65	1.93	7.42	3.14	4.82
13965	18474	5.47	5.85	0.75	0.869	4940	2.3	1.59	7.18	2.97	5.68
14668	19476	3.79	29.05	0.66	0.980	4950	3.1	1.65	7.55	1.79	3.50
14817	19656	4.61	10.69	0.80	1.115	4600	2.3	1.89	7.31	2.57	5.02
14838	19787	4.35	19.44	1.23	1.033	4875	3.05	1.68	7.59	2.15	3.32
15549	20644	4.47	5.09	0.90	1.555	4100	1.65	3.0	7.05	5.77	4.04
15696	20825	5.55	3.35	1.16	1.100	4775	2.55	2.18	7.32	9.43	5.36
15861	21017	5.50	14.18	0.98	1.190	4620	3.1	1.75	7.66	3.37	2.71
16335	21552	4.36	9.23	0.83	1.367	4215	2.05	1.87	7.29	2.21	4.27

Table 4. continued.

HIP	HD	V mag	plx mas	e.plx mas	B-V mag	T _{eff} K	log g dex	ξ kms ⁻¹	A(Fe)	$v \sin i$ kms ⁻¹	v_{macro} kms ⁻¹
16358	21755	5.93	6.31	0.96	0.953	5140	3.05	1.62	7.46	4.59	3.96
16780	22409	5.56	8.60	0.77	0.915	4980	2.8	1.51	7.18	3.33	3.58
16989	22675	5.86	8.35	0.74	0.980	5000	3.0	1.34	7.60	4.41	3.62
17103	22796	5.55	8.14	0.85	0.931	4990	3.0	1.6	7.33	2.15	5.78
18212	24240	5.76	7.58	0.78	1.040	4850	2.7	1.91	7.48	4.38	5.50
19009	25555	5.46	3.42	0.90	0.813	4360	1.53	1.68	7.16	5.78	6.67
19011	25723	5.62	8.12	0.84	1.062	4775	2.7	1.67	7.46	3.66	3.08
19388	26162	5.51	11.21	0.87	1.077	4800	2.9	1.7	7.55	4.00	3.14
19483	26409	5.44	8.65	0.82	0.941	5000	2.8	1.66	7.45	2.52	5.80
19996	27179	5.95	5.92	0.76	1.078	4850	2.6	1.77	7.55	5.79	5.50
20241	27278	5.95	9.42	0.79	0.962	4950	2.95	1.47	7.40	3.75	3.50
20250	27382	4.97	9.53	0.92	1.150	4550	2.5	1.57	7.17	0.94	4.92
20252	27348	4.93	14.42	0.83	0.950	5050	3.07	1.33	7.60	4.14	3.74
20268	27497	5.76	7.62	0.93	0.914	5180	3.2	1.37	7.63	0.88	6.15
20455	27697	3.77	21.29	0.93	0.983	5000	3.0	1.5	7.58	2.96	5.80
20732	28100	4.69	7.17	0.81	0.979	4930	2.45	1.77	7.25	4.96	5.66
20885	28307	3.84	20.66	0.85	0.952	5000	3.0	1.45	7.57	4.38	3.62
20889	28305	3.53	21.04	0.82	1.014	4910	2.75	1.73	7.54	3.66	5.62
21248	29085	4.49	26.22	0.71	0.972	4875	3.1	1.35	7.29	2.15	3.32
21421	29139	0.87	50.09	0.95	1.538	4100	1.70	2.45	7.13	5.20	4.04
21743	29737	5.56	10.34	0.69	0.926	4980	2.8	1.42	7.20	1.48	3.58
22220	30138	5.99	7.36	0.85	0.934	4920	2.9	1.71	7.43	2.98	5.64
22860	31414	5.71	6.85	0.63	0.953	5150	3.0	1.93	7.57	5.25	6.09
23015	31398	2.69	6.37	0.96	1.490	3950	1.15	2.57	7.31	7.32	3.75
23123	31767	4.47	3.42	0.86	1.369	4250	1.4	2.35	7.26	4.17	6.50
23685	32887	3.19	14.39	0.68	1.460	4150	1.8	2.2	7.30	4.30	4.14
24294	33833	5.90	7.31	0.74	0.960	4980	3.0	1.54	7.46	3.24	3.58
24822	34559	4.96	15.83	0.86	0.937	5060	3.1	1.53	7.52	3.02	3.77
25247	35369	4.13	18.71	0.74	0.943	4950	2.8	1.46	7.32	2.72	3.50
27280	38527	5.78	10.88	0.86	0.888	5125	3.05	1.32	7.42	1.71	6.04
27483	38656	4.51	15.34	0.80	0.949	4980	2.9	1.46	7.37	4.22	3.58
27588	39118	5.97	2.89	0.83	0.953	4550	1.52	2.16	7.15	4.19	6.97
27629	39004	5.60	8.66	0.98	0.978	5000	3.05	1.66	7.50	3.80	5.80
28812	41361	5.67	2.96	0.87	1.047	4900	2.4	1.95	7.38	3.88	7.53
28814	41380	5.63	1.31	0.76	1.041	4900	2.5	2.9	7.20	12.81	7.53
29379	42398	5.83	4.33	0.83	1.110	4650	2.4	1.54	7.34	4.20	2.78
29575	43023	5.83	10.36	0.73	0.910	5140	3.1	1.41	7.53	3.85	3.96
30457	44951	5.21	7.76	0.74	1.230	4500	2.4	1.92	7.26	3.76	4.82
30720	45433	5.55	4.35	0.86	1.376	4200	1.85	2.0	7.41	4.70	4.24
31159	46241	5.88	6.30	0.94	0.997	4925	2.7	1.59	7.42	3.87	3.44
31592	47205	3.95	50.41	0.70	1.037	4830	3.4	1.45	7.70	1.15	3.00
31700	47442	4.42	7.03	0.62	1.137	4550	2.3	1.8	7.40	4.31	4.92
32249	48433	4.49	11.82	0.83	1.167	4550	2.2	1.76	7.29	2.17	4.92
32562	48781	5.22	7.69	0.78	1.131	4725	2.5	1.82	7.41	2.55	5.26
32814	49738	5.68	2.17	0.88	1.329	4300	2.0	2.35	7.44	5.60	4.43
33152	50877	3.89	1.65	0.62	1.740	3900	0.65	4.0	7.17	12.31	5.95
33160	50778	4.08	12.94	0.87	1.418	4050	1.5	1.8	7.10	4.27	3.94
33421	51000	5.91	8.47	0.92	0.878	5180	3.05	1.55	7.45	2.26	6.15
33449	50522	4.35	19.14	0.76	0.850	4775	2.8	0.94	7.45	2.94	5.36
33856	52877	3.49	2.68	0.59	1.729	3850	1.05	3.5	7.20	10.76	3.55
33914	52556	5.78	5.06	0.85	1.140	4700	2.65	2.3	7.41	3.84	5.21
34033	52960	5.14	4.39	0.72	1.391	4150	1.8	2.0	7.41	5.33	4.14
34267	53329	5.55	10.68	0.88	0.909	4950	2.7	1.62	7.03	4.26	3.50
34387	54079	5.74	5.74	0.86	1.176	4450	2.1	1.8	7.07	3.04	4.72

Table 4. continued.

HIP	HD	V mag	plx mas	e.plx mas	B-V mag	T _{eff} K	log g dex	ξ kms ⁻¹	A(Fe)	$v \sin i$ kms ⁻¹	v_{macro} kms ⁻¹
34693	54719	4.41	10.81	0.97	1.261	4500	2.55	1.96	7.63	3.03	4.82
34987	55751	5.36	4.35	0.89	1.193	4550	2.1	1.86	7.38	3.74	4.92
35476	56989	5.90	6.27	0.85	1.069	4790	2.55	1.43	7.50	7.79	5.39
35615	57478	5.59	5.86	0.74	0.971	5090	2.65	1.94	7.41	8.40	7.83
35907	57669	5.23	4.48	0.96	1.249	4500	2.0	2.35	7.42	3.21	6.90
36041	58367	4.99	3.30	0.88	0.991	4900	2.05	2.04	7.37	4.22	7.53
36388	59311	5.60	2.00	0.94	1.493	4225	2.2	2.3	7.30	5.35	1.76
36616	59686	5.45	10.81	0.75	1.126	4650	2.75	1.68	7.64	4.28	2.78
36848	60666	5.78	10.41	0.67	1.045	4750	2.6	1.38	7.47	4.03	3.02
36962	60522	4.06	13.57	0.87	1.540	4130	1.9	2.6	7.13	5.19	4.10
37204	60986	5.58	10.65	0.97	0.921	5200	3.2	1.46	7.65	3.44	4.11
37364	61774	5.92	4.53	0.71	1.158	4680	2.45	1.58	7.43	1.78	5.17
37447	61935	3.94	22.61	0.80	1.022	4825	2.8	1.6	7.50	0.70	5.46
37740	62345	3.57	22.73	0.83	0.932	5030	2.95	1.58	7.47	4.36	3.70
37826	62509	1.16	96.74	0.87	0.991	4925	3.15	1.65	7.56	1.67	3.44
38253	63752	5.60	2.32	1.03	1.446	4075	1.0	2.38	7.14	6.21	6.22
38375	64152	5.62	11.90	0.73	0.956	4930	2.85	1.7	7.41	2.60	3.46
38962	65345	5.30	12.33	0.96	0.933	5020	3.02	1.34	7.55	3.41	3.67
39079	65695	4.93	13.06	0.96	1.205	4470	2.45	1.7	7.34	1.85	4.76
39177	65759	5.60	4.52	1.01	1.317	4300	2.05	1.9	7.55	5.73	4.43
39191	65714	5.87	2.90	0.89	1.021	4920	2.6	1.76	7.55	2.50	5.64
40107	68312	5.36	10.32	0.87	0.892	5150	3.2	1.44	7.47	2.25	3.99
40305	68077	5.88	6.59	0.73	1.016	4940	2.8	1.82	7.49	4.15	5.68
40526	69267	3.53	11.23	0.97	1.481	4200	2.05	2.3	7.30	4.88	4.24
40866	69994	5.80	6.39	0.82	1.137	4650	2.6	1.57	7.42	3.15	2.78
41075	70272	4.25	8.39	0.79	1.550	4175	2.05	2.8	7.25	5.41	4.19
41704	71369	3.35	17.76	0.65	0.856	5190	2.8	1.84	7.33	3.93	6.17
41909	72292	5.33	10.46	0.89	1.252	4450	2.55	1.68	7.64	2.89	4.72
42008	72561	5.89	0.60	1.09	1.066	4840	2.35	2.32	7.33	3.91	7.43
42402	73471	4.45	9.25	0.94	1.216	4550	2.4	2.1	7.54	2.95	4.92
42911	74442	3.94	23.97	0.83	1.083	4730	2.65	1.55	7.56	3.78	2.97
43409	75691	4.02	15.63	0.58	1.272	4450	2.55	1.7	7.47	2.21	4.72
43531	75506	5.15	11.91	0.72	0.971	4830	2.55	1.6	7.15	4.05	3.21
43813	76294	3.11	21.64	0.99	0.978	4840	2.55	1.73	7.33	3.18	5.49
43834	76219	5.23	5.68	0.84	1.000	4950	2.9	1.99	7.37	10.43	5.70
43923	76291	5.72	14.21	0.78	1.125	4665	3.0	1.63	7.42	2.02	2.82
44154	76813	5.23	10.19	0.75	0.913	5020	2.9	1.47	7.45	1.87	5.84
44356	77353	5.64	5.32	0.85	1.163	4525	2.15	1.89	7.11	3.04	4.87
44406	77445	5.85	4.91	0.91	1.100	4760	2.65	1.78	7.44	4.34	3.05
44659	77996	4.99	2.69	0.93	1.189	4380	1.75	1.88	7.37	2.32	6.71
44818	78235	5.42	12.56	0.81	0.888	5170	3.3	1.38	7.50	5.39	4.03
44936	78668	5.76	7.09	0.93	0.937	5000	2.65	1.39	7.42	3.72	5.80
45412	79452	5.98	7.17	0.90	0.839	5100	2.7	1.9	6.86	10.18	5.99
46390	81797	1.99	18.40	0.78	1.440	4200	2.15	2.5	7.44	6.20	1.70
46652	82087	5.87	6.33	0.90	1.032	4850	2.8	1.7	7.46	0.24	5.50
46750	82308	4.32	9.69	0.89	1.541	4000	1.3	2.3	7.19	6.12	3.85
46880	82734	5.02	9.76	0.69	1.023	4980	2.9	1.95	7.60	6.60	5.76
46952	82635	4.54	18.52	0.88	0.914	5150	3.5	1.55	7.51	6.59	3.99
46982	82870	5.56	4.79	0.83	1.159	4600	2.6	1.85	7.46	4.09	2.66
47029	82741	4.81	14.23	0.81	0.992	4910	2.9	1.62	7.32	3.88	3.41
47189	83189	5.73	3.42	0.93	1.223	4450	2.05	2.04	7.55	8.88	4.72
47431	83618	3.90	11.83	0.80	1.313	4400	2.35	1.9	7.42	2.43	4.63
47570	83805	5.61	9.59	0.74	0.951	5020	2.9	1.65	7.43	4.45	3.67
47959	84561	5.67	4.65	0.92	1.489	4225	2.05	2.23	7.17	3.50	4.29

Table 4. continued.

HIP	HD	V mag	plx mas	e.plx mas	B-V mag	T _{eff} K	log g dex	ξ kms ⁻¹	A(Fe)	$v \sin i$ kms ⁻¹	v_{macro} kms ⁻¹
48356	85444	4.11	11.92	0.81	0.918	5090	3.05	1.67	7.47	1.67	5.97
48455	85503	3.88	24.52	0.87	1.222	4565	2.9	1.95	7.78	5.06	2.58
48734	86080	5.85	4.84	0.78	1.129	4650	2.25	1.79	7.24	1.44	5.11
48802	85945	5.97	6.99	0.64	0.895	5160	3.15	1.47	7.53	7.53	6.11
50027	88547	5.77	6.19	0.89	1.178	4375	2.02	2.0	6.96	2.78	4.58
50336	89024	5.84	10.35	0.90	1.206	4755	3.2	2.6	7.28	4.60	3.03
51069	90432	3.83	13.14	0.79	1.456	4225	2.1	2.15	7.37	5.87	4.29
51775	91612	5.07	10.23	0.78	0.921	5025	2.95	1.42	7.38	4.03	3.68
52689	93291	5.49	11.34	0.86	0.908	5080	3.05	1.45	7.43	3.67	3.82
52943	93813	3.11	23.54	0.81	1.232	4435	2.2	2.0	7.24	1.76	4.70
53229	94264	3.79	33.40	0.78	1.040	4725	3.0	1.58	7.38	1.81	2.00
53261	94247	5.12	4.82	0.62	1.355	4385	2.3	2.2	7.28	3.61	4.60
53316	94481	5.65	7.97	0.83	0.832	5355	3.0	1.58	7.52	4.00	4.48
53740	95272	4.08	18.71	1.03	1.079	4785	2.95	1.75	7.50	3.76	5.38
53781	95212	5.47	3.70	0.78	1.466	4150	1.85	2.1	7.26	3.77	4.14
54539	96833	3.00	22.21	0.68	1.144	4655	2.55	2.0	7.35	3.38	2.79
55086	97989	5.88	7.74	0.73	1.102	4755	2.85	2.98	7.14	3.58	3.03
55282	98430	3.56	16.75	0.82	1.112	4580	2.35	1.9	7.06	2.40	4.98
55650	99055	5.39	8.93	0.83	0.938	5020	2.7	1.71	7.34	4.52	3.67
55716	99196	5.80	6.97	0.85	1.376	4215	1.75	2.1	7.14	4.26	4.27
55797	99283	5.73	9.38	0.71	0.988	4930	2.85	1.67	7.31	4.28	3.46
55945	99648	4.95	5.25	0.84	1.000	4950	2.52	1.87	7.42	4.40	5.70
56647	100920	4.30	18.31	0.89	0.983	4910	2.8	1.61	7.33	4.27	3.41
57399	102224	3.69	16.64	0.60	1.181	4495	2.1	2.05	7.05	1.18	4.81
58181	103605	5.83	10.34	0.63	1.101	4630	2.6	1.9	7.32	3.18	5.08
58654	104438	5.59	9.01	0.77	1.019	4875	3.0	1.64	7.43	3.64	3.32
58948	104979	4.12	19.08	0.77	0.967	4950	2.77	1.68	7.07	1.55	5.70
59316	105707	3.02	10.75	0.71	1.326	4475	2.3	2.9	7.31	5.28	4.77
59501	106057	5.60	6.73	0.74	0.961	5000	2.95	1.68	7.41	3.19	3.62
59847	106714	4.93	13.12	0.88	0.957	4850	2.8	1.87	7.29	2.14	5.50
60202	107383	4.72	9.04	0.86	1.010	4880	3.0	1.67	7.25	0.60	5.56
60485	107950	4.76	8.30	0.58	0.877	5100	2.5	1.7	7.37	5.47	7.84
60646	108225	5.01	14.35	0.60	0.955	5050	3.0	1.5	7.57	4.39	3.74
60742	108381	4.35	19.18	0.83	1.128	4675	2.55	1.68	7.65	3.52	2.84
61420	109519	5.86	5.00	0.84	1.242	4495	2.5	2.65	7.30	5.42	4.81
61571	109742	5.70	6.29	0.85	1.436	4280	2.15	2.25	7.36	4.22	4.39
62103	110646	5.91	14.26	0.77	0.850	5000	3.07	1.29	7.01	1.59	3.62
63533	113095	5.97	8.14	0.78	0.971	4975	2.95	1.57	7.45	1.49	5.75
63608	113226	2.85	31.90	0.87	0.934	5115	3.1	1.71	7.58	1.69	6.02
64078	114038	5.15	10.66	0.84	1.138	4715	2.8	1.69	7.55	1.33	5.24
64540	115004	4.94	6.24	0.68	1.061	4730	2.4	1.91	7.39	7.50	5.27
64823	115478	5.33	10.94	1.00	1.304	4350	2.6	1.76	7.59	4.88	2.06
64962	115659	2.99	24.69	0.70	0.920	5110	2.9	1.55	7.52	3.35	6.01
65301	116292	5.36	10.20	0.73	0.987	4940	2.75	1.55	7.42	2.26	5.68
65323	116365	5.88	2.81	0.86	1.431	4180	1.9	2.06	7.16	4.87	4.20
66098	117818	5.21	12.36	0.78	0.964	4900	2.7	1.63	7.18	3.87	3.38
66320	118219	5.70	8.80	0.76	0.950	4915	2.7	1.55	7.24	1.37	5.63
66907	119458	5.98	6.71	0.76	0.857	5125	3.0	1.66	7.40	4.05	6.04
67210	120048	5.92	8.08	0.63	0.948	5100	3.15	1.48	7.55	2.58	5.99
67459	120477	4.05	13.29	0.81	1.520	4170	1.60	2.60	6.92	5.06	4.18
67545	120602	6.00	8.09	0.81	0.899	5140	2.88	1.59	7.35	3.82	6.07
68895	123123	3.25	32.17	0.77	1.091	4670	2.65	1.8	7.33	2.25	2.83
69427	124294	4.18	14.59	0.95	1.323	4175	1.6	1.9	7.02	4.13	4.19
69673	124897	-0.05	88.85	0.74	1.239	4230	1.65	1.95	6.86	3.80	4.30

Table 4. continued.

HIP	HD	V mag	plx mas	e_plx mas	B-V mag	T _{eff} K	log g dex	ξ kms ⁻¹	A(Fe)	$v \sin i$ kms ⁻¹	v_{macro} kms ⁻¹
70469	126218	5.34	8.16	0.87	0.962	5125	3.0	1.72	7.64	4.59	3.93
70791	127243	5.58	10.59	0.61	0.864	5030	2.7	2.05	6.79	3.99	3.70
71053	127665	3.57	21.92	0.81	1.298	4385	2.3	2.17	7.30	3.14	4.60
71832	129312	4.86	5.66	0.82	0.992	4925	2.6	1.74	7.39	8.42	5.65
71837	129336	5.55	8.46	0.86	0.941	4980	2.9	1.67	7.22	3.41	3.58
72125	129972	4.60	14.48	0.79	0.972	4980	2.9	1.72	7.43	0.80	5.76
72210	129944	5.80	8.91	0.96	0.980	4865	2.7	1.8	7.19	4.02	3.30
72571	130694	4.42	10.68	0.83	1.366	4250	2.0	2.13	6.80	4.23	4.33
72934	131530	5.78	8.94	0.96	0.982	5015	3.2	1.49	7.53	0.85	5.83
73133	131918	5.48	6.06	0.79	1.491	4140	1.65	2.25	7.25	4.96	4.12
73166	132146	5.72	5.28	0.81	0.951	5075	2.8	1.84	7.46	2.83	5.94
73555	133208	3.49	14.91	0.57	0.956	5100	2.8	1.8	7.49	2.64	5.99
73620	133165	4.39	17.78	0.90	1.026	4700	2.7	1.9	7.19	2.24	2.90
73909	134190	5.24	12.53	0.53	0.958	4830	2.4	1.7	7.02	3.45	3.21
74239	134373	5.75	7.25	1.00	1.045	4900	2.85	2.0	7.45	4.26	5.60
74666	135722	3.46	27.94	0.61	0.961	4900	2.75	1.65	7.11	2.87	3.38
74732	135534	5.52	6.52	1.16	1.357	4365	2.25	1.92	7.56	4.24	4.56
75352	136956	5.72	5.41	0.77	1.039	5040	2.9	1.67	7.60	2.55	5.88
75458	137759	3.29	31.92	0.51	1.166	4605	2.95	1.73	7.60	3.93	2.67
75730	137744	5.64	3.59	0.93	1.545	4230	2.05	2.25	7.29	5.10	4.30
75944	138137	5.82	5.78	0.83	1.056	4935	2.75	1.98	7.45	3.36	5.67
76425	139195	5.26	13.89	0.70	0.925	5000	3.15	1.56	7.37	3.56	3.62
76810	140027	6.00	7.24	0.79	0.908	5215	3.1	1.61	7.48	4.50	4.14
77512	141714	4.59	19.71	0.73	0.794	5300	3.35	1.48	7.23	5.62	4.35
77738	142531	5.81	9.09	0.51	0.972	5000	3.15	1.52	7.58	3.07	3.62
77853	142198	4.13	20.02	0.88	1.003	4685	2.2	1.67	7.14	3.06	5.18
78132	142980	5.54	14.36	0.80	1.141	4610	2.95	1.76	7.46	4.58	2.68
78442	143553	5.82	13.62	0.79	1.003	4810	3.10	1.33	7.34	3.01	3.17
78990	144608	4.31	12.32	0.89	0.831	5320	2.75	1.85	7.44	3.50	6.42
79195	145206	5.39	6.60	0.91	1.446	4160	1.95	2.65	7.23	2.91	4.16
79540	145897	5.24	7.43	0.91	1.394	4350	2.45	1.87	7.48	3.98	2.06
79882	146791	3.23	30.34	0.79	0.966	4970	2.9	1.52	7.42	3.50	3.55
80331	148387	2.73	37.18	0.45	0.910	5110	3.15	1.55	7.48	3.69	3.89
80343	147700	4.48	18.32	0.89	0.996	4775	2.55	1.71	7.29	1.72	5.36
80693	148513	5.41	7.72	0.87	1.461	4200	2.05	2.15	7.47	3.21	4.24
80894	148786	4.29	15.53	0.77	0.924	5175	3.1	1.68	7.65	5.01	6.14
81660	151101	4.84	4.79	0.45	1.212	4535	2.1	2.28	7.36	1.17	6.95
81724	150416	4.91	8.34	0.85	1.095	5000	2.6	1.86	7.36	5.19	7.69
81833	150997	3.48	29.11	0.52	0.916	5020	3.0	1.43	7.29	2.47	5.84
83000	153210	3.19	37.99	0.75	1.160	4655	2.7	1.82	7.56	2.16	5.12
83254	153834	5.69	1.07	0.74	1.332	4340	1.7	2.61	7.34	5.23	6.64
84380	156283	3.16	8.89	0.52	1.437	4170	1.9	2.26	7.50	6.12	4.18
84671	156681	5.03	4.72	0.80	1.539	4170	2.1	2.25	7.28	5.47	1.62
84950	157681	5.69	5.52	0.51	1.463	4255	2.05	2.18	7.30	3.78	4.34
85139	157617	5.77	3.03	0.79	1.251	4565	2.2	2.47	7.46	7.34	4.95
85355	157999	4.34	2.78	0.92	1.480	4080	1.52	2.54	7.42	7.51	4.00
85693	158899	4.41	8.88	0.64	1.434	4325	2.55	2.62	7.40	6.22	2.00
85715	158974	5.63	8.65	0.56	0.960	5090	3.15	1.57	7.58	2.01	5.97
85888	159501	5.72	8.62	0.53	1.089	4685	2.65	1.77	7.20	0.94	2.86
86742	161096	2.76	39.78	0.75	1.168	4680	2.95	2.02	7.62	3.84	2.85
87808	163770	3.86	4.87	0.54	1.350	4255	1.25	2.75	7.38	7.45	6.51
87847	163532	5.44	7.66	0.71	1.162	4800	2.8	1.98	7.42	1.46	5.41
87933	163993	3.70	24.12	0.52	0.935	5085	3.20	1.8	7.49	4.53	3.83
88048	163917	3.32	21.35	0.79	0.987	4900	2.85	2.05	7.55	3.04	5.60

Table 4. continued.

HIP	HD	V mag	plx mas	e.plx mas	B-V mag	T _{eff} K	log g dex	ξ kms ⁻¹	A(Fe)	$v \sin i$ kms ⁻¹	v_{macro} kms ⁻¹
88636	165683	5.72	4.69	0.62	1.179	4600	2.35	2.05	7.37	1.39	5.02
88684	165438	5.74	28.61	0.83	0.968	4955	3.60	1.22	7.60		
88765	165760	4.64	13.71	0.82	0.951	5025	3.0	1.75	7.45	1.02	5.85
88839	165634	4.55	9.38	0.77	0.938	4980	2.65	1.73	7.44	1.49	3.58
89008	166640	5.57	7.52	0.57	0.915	5080	3.0	1.54	7.50	1.80	5.95
89587	167768	5.99	9.91	0.83	0.890	4930	2.5	2.05	6.72	4.42	7.58
89826	168775	4.33	13.71	0.56	1.162	4590	2.50	1.7	7.64	2.81	5.00
89919	B+62 1612	8.88	3.81	0.80	1.058	5130	3.1	1.6	7.41		
89962	168723	3.23	52.81	0.75	0.941	4955	3.2	1.33	7.34	0.44	3.52
90067	169191	5.25	7.48	0.66	1.250	4515	2.65	1.75	7.44	0.95	4.85
90139	169414	3.85	25.40	0.65	1.168	4585	3.0	1.45	7.56	3.48	2.62
90496	169916	2.82	42.20	0.90	1.025	4770	2.9	1.45	7.44	3.81	3.07
91004	171115	5.49	0.95	0.97	1.795	3835	0.25	3.1	7.03	7.31	5.85
91105	171391	5.12	11.25	0.78	0.926	5125	3.15	1.55	7.47	3.05	6.04
91117	171443	3.85	18.72	0.81	1.317	4280	2.15	1.88	7.51	4.58	4.39
92747	174947	5.68	1.88	0.85	1.206	4685	2.10	2.48	7.38	3.82	7.19
93026	175751	4.83	15.77	0.89	1.057	4730	2.85	1.85	7.46	3.00	2.97
93085	175775	3.52	8.76	0.99	1.151	4595	2.4	2.1	7.48	6.29	5.01
93429	176678	4.02	21.95	0.92	1.079	4690	2.95	1.53	7.51	3.91	2.88
93864	177716	3.32	27.09	1.48	1.169	4690	3.2	3.9	7.22	1.04	4.90
94302	180006	5.13	9.57	0.47	1.008	4940	2.9	1.54	7.58	5.00	5.68
94624	180262	5.58	5.32	0.90	1.067	4960	2.6	1.77	7.49	5.48	5.72
94779	181276	3.80	26.48	0.49	0.950	5050	3.25	1.65	7.58	4.28	3.74
94820	180540	4.88	6.09	0.86	1.013	4850	2.2	1.95	7.31	4.08	7.45
95352	182694	5.85	8.06	0.47	0.924	5115	3.1	1.59	7.48	3.20	6.02
95785	183491	5.82	6.74	0.72	1.023	4890	2.85	1.64	7.57	2.80	5.58
96229	184406	4.45	29.50	0.78	1.176	4670	3.2	1.82	7.53	2.78	2.83
96327	184492	5.12	7.34	0.76	1.122	4875	2.5	2.16	7.33	8.88	7.49
96459	185351	5.17	24.64	0.49	0.928	5050	3.55	1.46	7.49	2.06	3.00
96516	185194	5.67	6.89	0.72	1.007	4975	2.7	1.74	7.51	3.32	5.75
97118	186675	4.89	11.70	0.50	0.948	5050	2.85	1.65	7.47	2.94	5.89
97402	187193	6.00	8.16	0.72	0.993	4930	2.95	1.52	7.38	1.24	5.66
98337	189319	3.51	11.90	0.71	1.571	4150	1.70	2.85	7.09	5.81	4.14
98571	190147	5.06	7.60	0.47	1.122	4700	2.5	1.95	7.38	3.63	5.21
98823	190327	5.51	6.19	0.79	1.063	4850	2.7	1.98	7.34	10.30	5.50
99951	192944	5.30	6.91	0.64	0.951	5000	2.7	1.68	7.39	5.02	5.80
100064	192947	3.58	30.01	0.91	0.883	5035	1.75	2.62	7.34	7.79	7.74
100587	194317	4.43	12.77	0.62	1.331	4435	2.7	2.0	7.53	4.85	2.26
100754	194577	5.68	6.00	0.73	0.921	5075	3.0	1.47	7.51	4.65	5.94
101870	196753	5.91	1.65	0.74	0.953	4550	1.65	2.3	7.13	6.20	6.97
101986	197139	5.97	6.93	0.54	1.186	4485	2.4	1.44	7.41	6.39	4.79
102422	198149	3.41	69.73	0.49	0.912	4985	3.45	1.34	7.31	1.04	2.00
102453	197912	4.22	15.84	0.62	1.051	4940	3.17	1.87	7.46	4.31	3.48
102488	197989	2.48	45.26	0.53	1.021	4785	2.75	1.62	7.38	3.01	3.11
102978	198542	4.12	5.19	0.95	1.633	3960	0.85	2.9	6.88	4.68	6.04
103294	199253	5.19	6.88	0.74	1.119	4625	2.35	1.75	7.30	4.80	5.07
103360	199612	5.92	2.56	0.52	1.054	4740	2.6	2.0	7.40	4.76	5.29
104060	200905	3.72	2.77	0.52	1.609	3920	1.00	3.1	7.08	9.30	3.69
104459	201381	4.50	19.93	0.77	0.926	5025	3.10	1.5	7.48	3.29	3.68
104963	202320	5.17	4.72	0.82	1.161	4515	1.85	2.07	7.23	4.14	6.92
105412	203222	5.87	9.69	0.86	0.912	5050	3.05	1.46	7.50	1.79	5.89
105497	203644	5.68	9.93	0.55	1.100	4740	2.75	1.77	7.53	4.25	5.29
105515	203387	4.28	15.13	0.80	0.888	5025	3.0	1.48	7.34	5.67	5.85
106039	204381	4.50	18.18	0.89	0.889	5155	3.30	1.78	7.47	5.74	4.00

Table 4. continued.

HIP	HD	V mag	plx mas	e.plx mas	B-V mag	T _{eff} K	log g dex	ξ kms ⁻¹	A(Fe)	$v \sin i$ kms ⁻¹	v_{macro} kms ⁻¹
106481	205435	3.98	26.20	0.51	0.885	5125	3.25	1.46	7.34	4.26	3.93
107188	206453	4.72	11.22	0.79	0.868	5040	2.65	1.72	7.10	3.72	5.88
107315	206778	2.38	4.85	0.84	1.520	4150	1.25	3.5	7.31	8.32	6.34
107382	206834	5.10	4.08	0.89	1.108	4815	2.35	2.63	7.30	3.75	7.39
108691	209128	5.60	4.93	0.83	1.279	4465	2.60	2.18	7.40	4.04	4.75
109023	209761	5.75	8.22	0.73	1.249	4420	2.35	1.73	7.41	5.19	4.67
109068	209747	4.86	12.38	0.90	1.443	4130	1.90	2.03	7.51	4.77	4.10
109492	210745	3.39	4.49	0.50	1.558	4120	0.75	3.4	7.27	10.64	6.30
109602	210762	5.97	1.07	0.70	1.500	4185	1.65	2.45	7.49	7.87	4.21
109754	211073	4.50	5.79	0.64	1.385	4360	2.45	2.77	7.40	6.50	2.08
109937	211388	4.14	5.20	0.61	1.447	4260	2.15	2.7	7.50	7.60	4.35
109972	211554	5.88	4.48	0.56	0.950	5075	2.8	1.84	7.57	5.21	5.94
110000	211361	5.34	6.74	0.88	1.132	4800	2.9	1.83	7.48	3.43	5.41
110003	211391	4.17	17.04	0.74	0.979	5000	3.1	1.67	7.56	3.94	3.62
110023	211434	5.75	9.56	0.86	0.878	5025	2.7	1.6	7.18	1.96	5.85
110532	212320	5.92	7.10	0.93	0.998	5030	2.9	1.95	7.22	2.89	5.86
110602	212430	5.76	6.01	0.76	0.970	4975	2.75	1.73	7.28	4.07	3.56
110986	213119	5.60	5.63	0.85	1.578	4090	1.65	2.5	7.01	5.01	4.02
111362	213930	5.72	9.60	0.53	0.966	4975	3.05	1.61	7.54	5.18	5.75
111394	213789	5.88	7.35	0.86	0.977	5015	3.0	1.66	7.39	3.80	5.83
111925	214878	5.94	9.49	0.54	0.946	5050	3.15	1.49	7.53	3.86	3.74
111944	214868	4.50	10.81	0.56	1.318	4445	2.50	2.05	7.32	1.80	4.71
112067	214995	5.92	12.22	0.79	1.114	4680	2.70	1.8	7.45	7.21	5.17
112242	215373	5.11	11.89	0.60	0.960	4950	2.87	1.69	7.50	3.61	5.70
112440	215665	3.97	8.26	0.70	1.070	4650	2.0	1.89	7.23	8.03	7.13
112529	215721	5.24	12.26	0.87	0.941	4900	2.6	1.86	7.01	3.90	3.38
112724	216228	3.50	28.27	0.52	1.053	4830	3.00	1.59	7.54	3.27	3.21
112748	216131	3.51	27.95	0.77	0.933	4980	2.9	1.51	7.39	0.20	5.76
113084	216646	5.82	9.63	0.79	1.136	4600	2.65	1.65	7.56	3.05	2.66
113562	217303	5.66	4.62	0.71	1.253	4250	1.50	1.76	6.75	3.86	4.33
113622	217459	5.85	5.96	0.80	1.343	4260	2.05	1.84	7.36	2.51	4.35
113686	217563	5.94	1.23	0.91	0.992	4950	2.0	2.27	7.36	2.14	7.61
113864	218029	5.25	8.48	0.52	1.248	4450	2.4	1.78	7.68	3.18	4.72
114341	218594	3.68	13.96	0.94	1.202	4435	2.15	2.09	7.29	3.59	4.70
114449	218792	5.68	6.45	0.81	1.330	4330	2.55	1.91	7.51	4.12	2.01
114855	219449	4.24	21.97	0.89	1.107	4715	2.70	1.73	7.46	2.78	5.24
114971	219615	3.70	24.92	0.89	0.916	4940	2.9	1.76	6.95	4.20	3.48
115152	219945	5.44	9.95	0.63	1.014	4880	2.85	1.55	7.40	1.21	5.56
115438	220321	3.96	20.14	0.72	1.082	4655	2.65	1.59	7.23	3.08	2.79
115669	220704	4.38	10.57	0.72	1.460	4150	1.8	2.34	7.22	3.90	4.14
115830	220954	4.27	20.54	0.80	1.062	4775	2.95	1.84	7.51	1.79	3.08
117375	223252	5.49	11.19	0.85	0.941	5000	3.0	1.6	7.41	2.57	5.80
117567	223559	5.70	7.09	0.92	1.488	4090	1.20	2.25	6.93	3.44	4.02
117756	223807	5.76	5.33	0.81	1.171	4605	2.65	1.89	7.47	3.60	2.67
118209	224533	4.88	14.58	0.83	0.930	5115	3.3	1.56	7.47	4.64	3.90